A Dynamic One-D Implementation of a GEC Heating Model for Hot Jupiters

Derek L. Buzasi
Florida Gulf Coast University

Introduction

Hot Jupiters frequently have radii which are "inflated" relative to the expected mass-radius relation (Fortney & Nettleman 2010). The degree of inflation

- is correlated with orbital semimajor axis (Demory & Seager 2011, Weiss et al. 2013)
- becomes significant for $a \approx r_{Alfven}$
- appears dependent on stellar activity level (Buzasi 2013)

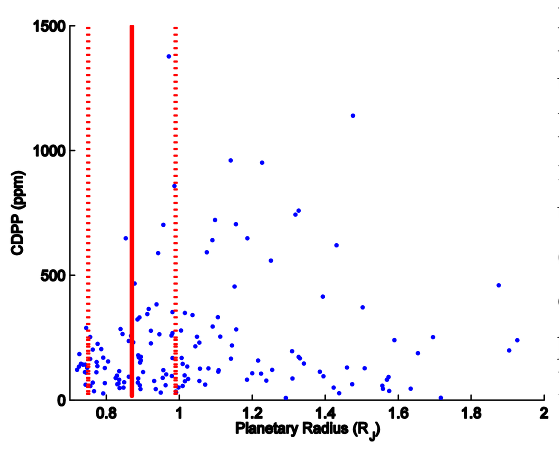

Figure 1. Radius vs. activity for Kepler hot Jupiters, with CDPP used as a stellar activity proxy. Red vertical lines show the independently-determined uninflated radius with errors (Demory & Seager 2011). The difference between the populations on both sides of the line is statistically significant.

Model Physics & Geometry

The model calculated currents internal to the planet generated by the electric field produced by stellar wind/magnetosphere interaction and mapped down to ionosphere.

•Stellar wind ~ solar wind

•Planetary model includes Alexander & Ferguson (1994) opacity, Militzer & Hubbard (2013) equation of state

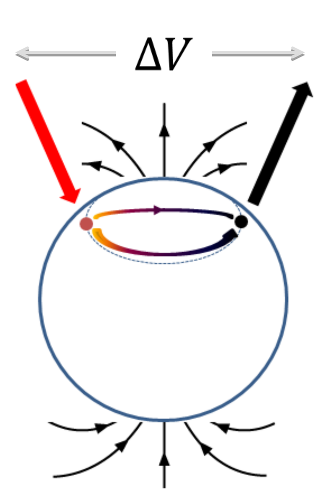

Figure 2. The presence of a ~10 G planetary magnetic field renders conductivity inhomogeneous. We assume that the magnetic dipole moment is coaligned with the rotation axis and ecliptic poles. The potential difference across ionosphere drives Pedersen ($\perp$ to $\vec{B}$) and parallel currents. The resulting predominantly radial current flow mirrors the global electric circuit (GEC) seen on Earth, but on a much larger scale.

Results

Ionization levels were calculated using a simplified Saha equation (Menou 2012)

$$\frac{x_j^2}{1-x_j^2} \cong \frac{1}{n_j kT}\left(\frac{2\pi m_e}{h^2}\right)^{3/2} (kT)^{5/2} \exp\left(-I_j/kT\right)$$

where n_j and I_j are the relative abundances and ionization potentials of element j; the first 28 elements were used. The resulting electron densities were used to calculate the classical (σ_0), Pedersen (σ_P), and Hall (σ_H) conductivities. For example,

$$\sigma_P = \sigma_0 \frac{\nu_{ei}^2}{\nu_{ei}^2 + \Omega_e^2}$$

where ν_{ei}^2 is the electron-ion collision rate and Ω_e the electron gyrofrequency (Figure 3).

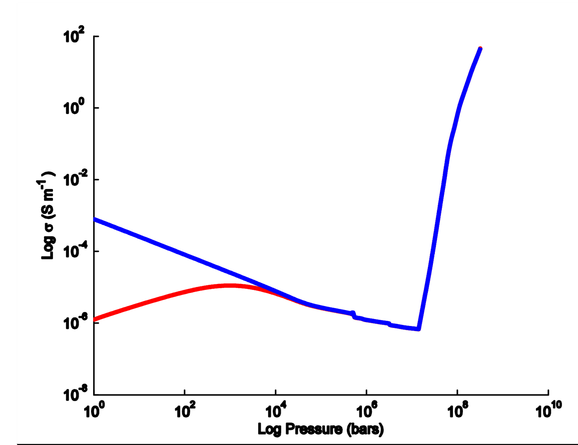

Figure 3: Classical (blue) and Pedersen (red) conductivity as a function of pressure for a $1M_J$ model with $B = 10$G located at $a = 0.08$AU. Pedersen conductivity drops dramatically in the outer layers, limiting heating in that region.

The ionospheric electric potential was taken as zero except at rings located along the invariant latitude

$$\Lambda = cos^{-1}\left(\sqrt{\frac{R_{PL}}{R_M}}\right)$$

At those points the potential values adopted were those of the wind-induced field $E = v_w B_w R_M \sin\varphi$.

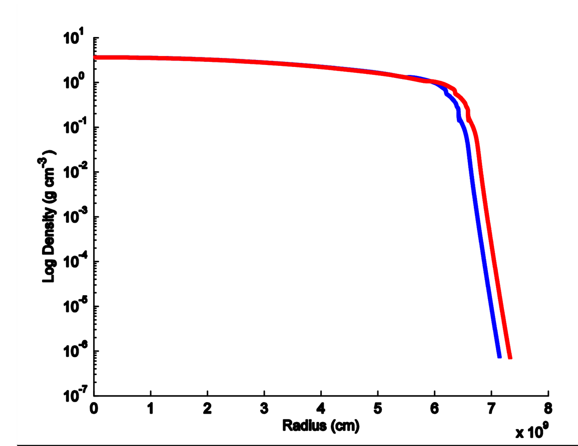

Figure 4: Density profiles for a model with (red) and without (blue) GEC heating. This 10G model is located at $a = 0.06$ AU.

Internal current densities and Joule heating rates were then calculated, interiors models updated, and new conductivity profiles determined. The process was repeated iteratively until convergence.

Energy deposition for a typical model is shown in Figure 5. Total heating is generally limited by the power available from the wind rather than by the wind-induced field strength.

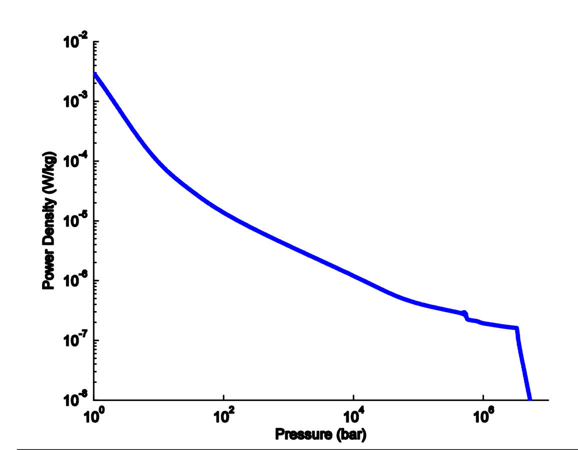

Figure 5: Heating rate as a function of pressure for a $1M_J$ model at $a = 0.06$ AU.

Conclusions

Successful models which account for the observed radius excess in hot Jupiters by additional heating must be capable of supplying $\sim 10^{27}$ erg s^{-1} to the convective portion of the planetary interior, which for the archetypical hot Jupiter at $a = 0.08$ AU lies at about $P = 1$kbar. The proposed model is capable of such heating. In addition, the model becomes efficient at heating the planetary interior for $a \leq 0.1$AU and suggests that heating should be correlated with both stellar and planetary magnetic fields.

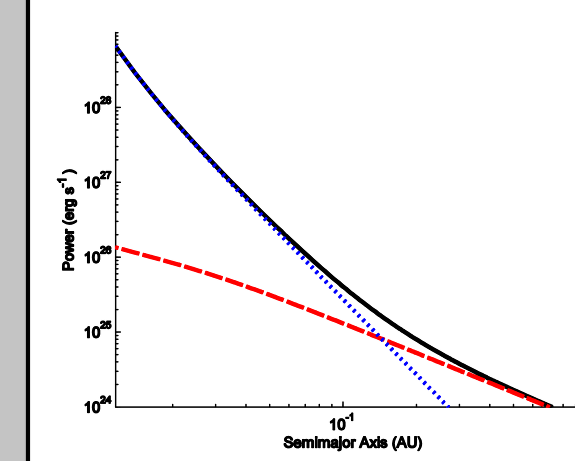

Figure 6: Maximum power available for planetary heating from a solar-like wind interacting with a 10G planetary field. Components shown include kinetic (red), magnetic (blue), and total (black).

It is likely that multiple heating models coexist, including tidal heating (for noncircular orbits) and Ohmic heating (Batygin & Stevenson 2010, Batygin et al. 2011). The model proposed here may complement the latter.

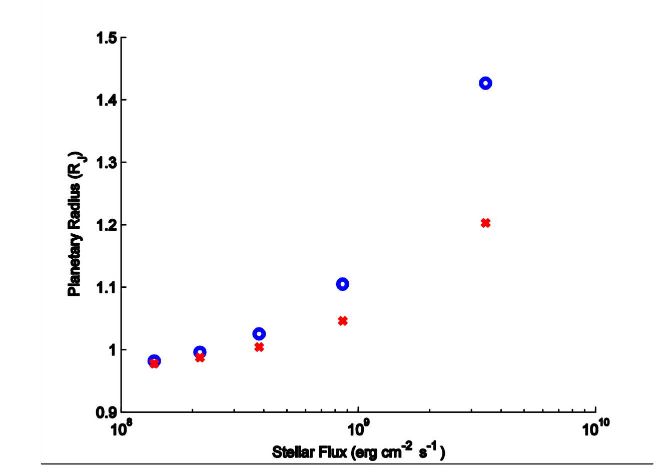

Figure 7: Planetary radius as a function of stellar flux, assuming a solar-like host star. Results for both the 1G (red) and 10G (blue) cases are shown.

Acknowledgments

I am grateful to the Whitaker Foundation for its support of the Whitaker Chair at Florida Gulf Coast University. Funding for the *Kepler* mission is provided by the NASA Science Mission Directorate, and this work was in part funded by the *Kepler* Participating Science Program grant NNH09CE70C.

References

Akasofu, S. I. 1981, Space Sci. Rev., 28, 121.
Alexander, D. R. & Ferguson, J. W. 1994, ApJ, 437, 879.
Batygin, K. & Stevenson, D. J. 2010, ApJL, 714, 238.
Batygin, K., Stevenson, D. J. & Bodenheimer, P. H. 2011, ApJ, 738, 1
Buzasi, D., 2013, ApJL, 765, 25.
Demory, B.-O. & Seager, S. 2011, ApJS, 197, 12.
Fortney, J. J. & Nettlemann, N. 2010, Space Sci. Rev., 152, 423.
Menou, K. 2012, ApJL, 754, 9.
Militzer, B. & Hubbard, W. , 2013, ApJ, 774, 148.
Paxton, B. et al. 2011, ApJS, 192, 3.

Next Steps

Further improvements planned include incorporating:

•Self-consistent models using MESA (Paxton et al. 2011) that incorporate GEC heating into structure calculations.

•Auroral precipitation and its effect on conductivity

•GEC model interactions with other heating mechanisms, including Ohmic (Batygin et al. 2011) and tidal heating.

•Observational tests